Title
The analysis here of 74 obsidian artifacts from Elmer's site in Safford Valley, southeastern Arizona is dominated by obsidian from the Mule Creek Source Complex in eastern New Mexico, a few samples from the Cow Canyon source of eastern Arizona, one a...

Author
Shackley, M. Steven

Publication Date
2019-04-02

GEOARCHAEOLOGICAL XRF LAB
A GREEN SOLAR FACILITY

GEOARCHAEOLOGICAL X-RAY FLUORESCENCE SPECTROMETRY LABORATORY
8100 WYOMING BLVD., SUITE M4-158 ALBUQUERQUE, NM 87113 USA

SOURCE PROVENANCE OF OBSIDIAN ARTIFACTS FROM ELMER'S SITE, SAFFORD VALLEY, SOUTHEASTERN ARIZONA

by

M. Steven Shackley Ph.D., Director
Geoarchaeological XRF Laboratory
Albuquerque, New Mexico

Report Prepared for

Dr. Jeff Clark
Archaeology Southwest
Tucson, Arizona

2 April 2019

INTRODUCTION

The analysis here of 74 obsidian artifacts from Elmer's site in Safford Valley, southeastern Arizona is dominated by obsidian from the Mule Creek Source Complex in eastern New Mexico, a few samples from the Cow Canyon source of eastern Arizona, one artifact produced from the Government Mountain source in northern Arizona, and four sources that do not match any known source in western North America (see Tables 1 and 2 and Figures 1 and 2). Antelope Creek at Mule Creek and Cow Canyon, both sources part of the Mogollon-Datil Volcanic Province in western New Mexico and eastern Arizona, are dominant sources in Late Classic sites throughout the Southwest, and can be found as secondary deposits in San Francisco and Gila River Quaternary alluvium (Mills et al. 2013; Shackley et al. 2018). Government Mountain obsidian has been recovered in the assemblages from Fort Apache sites as well (see Shackley 2016).

While the Mule Creek and Cow Canyon sources can be found as secondary deposits in Gila River Quaternary alluvium, many of the bipolar cores and flakes in this assemblage appear to have primary cortex, including the silver sheen found at the primary sources that does not survive the erosional process. It is likely that many of the artifacts here were produced from obsidian from the primary source localities. The four artifacts that could not be assigned to source have not been seen in other sites in the area, and they do not match any of the known sources in the Skinner/Shackley database that contains 260 obsidian sources or source groups in western North America. It is possible that it is a source in the region, but it is not one of the reported "unknown" sources (see Shackley 1998, 2005).

LABORATORY SAMPLING, ANALYSIS AND INSTRUMENTATION

All archaeological samples are analyzed whole. The results presented here are quantitative in that they are derived from "filtered" intensity values ratioed to the appropriate x-ray continuum regions through a least squares fitting formula rather than plotting the proportions of the net intensities in a ternary system (McCarthy and Schamber 1981; Schamber 1977). Or more essentially, these data through the analysis of international rock standards, allow for inter-instrument comparison with a predictable degree of certainty (Hampel 1984; Shackley 2011).

All analyses for this study were conducted on a ThermoScientific *Quant'X* EDXRF spectrometer, located in the Geoarchaeological XRF Laboratory, Albuquerque, New Mexico. It is equipped with a thermoelectrically Peltier cooled solid-state Si(Li) X-ray detector, with a 50 kV, 50 W, ultra-high-flux end window bremsstrahlung, Rh target X-ray tube and a 76 µm (3 mil) beryllium (Be) window (air cooled), that runs on a power supply operating 4-50 kV/0.02-1.0 mA at 0.02 increments. The spectrometer is equipped with a 200 l min^{-1} Edwards vacuum pump, allowing for the analysis of lower-atomic-weight elements between sodium (Na) and titanium (Ti). Data acquisition is accomplished with a pulse processor and an analogue-to-digital converter. Elemental composition is identified with digital filter background removal, least squares empirical peak deconvolution, gross peak intensities and net peak intensities above background.

The analysis for mid Zb condition elements Ti-Nb, Pb, Th, the x-ray tube is operated at 30 kV, using a 0.05 mm (medium) Pd primary beam filter in an air path at 100 seconds livetime to generate x-ray intensity $K\alpha_1$-line data for elements titanium (Ti), manganese (Mn), iron (as $Fe_2O_3^T$), cobalt (Co), nickel (Ni), copper, (Cu), zinc, (Zn), gallium (Ga), rubidium (Rb), strontium (Sr), yttrium (Y), zirconium (Zr), niobium (Nb), lead (Pb), and thorium (Th). Not all these elements are reported since their values in many volcanic rocks are very low. Trace element intensities were converted to concentration estimates by employing a least-squares calibration line ratioed to the Compton scatter established for each element from the analysis of international rock standards certified by the National Institute of Standards and Technology (NIST), the US. Geological Survey (USGS), Canadian Centre for Mineral and Energy Technology, and the Centre de Recherches Pétrographiques et Géochimiques in France (Govindaraju 1994). Line fitting is linear (XML) for all elements but Fe where a derivative fitting is used to improve the fit for iron and thus for all the other elements. When barium (Ba) is analyzed in the High Zb condition, the Rh tube is operated at 50 kV and up to 1.0 mA, ratioed to the bremsstrahlung region (see Davis 2011; Shackley 2011). Barium was acquired for a number of artifacts to increase source assignment confidence, such as the Mule Mountain source that can be confused with the Nutt Mountain source located in Sierra County, New Mexico (see Shackley et al. 2018). Further details concerning the petrological choice of these elements in Southwest obsidians is available in Shackley (1988, 1995, 2005; also Mahood and Stimac 1991; and Hughes and Smith 1993). Nineteen specific pressed powder standards are used for the best fit regression calibration for elements Ti-Nb, Pb, Th, and Ba, include G-2 (basalt), AGV-2 (andesite), GSP-2 (granodiorite), SY-2 (syenite), BHVO-2 (hawaiite), STM-1 (syenite), QLO-1 (quartz latite), RGM-1 (obsidian), W-2 (diabase), BIR-1 (basalt), SDC-1 (mica schist), TLM-1 (tonalite), SCO-1 (shale), NOD-A-1 and NOD-P-1 (manganese) all US Geological Survey standards, NIST-278 (obsidian), U.S. National Institute of Standards and Technology, BE-N (basalt) from the Centre de Recherches Pétrographiques et Géochimiques in France, and JR-1 and JR-2 (obsidian) from the Geological Survey of Japan (Govindaraju 1994).

The data from the WinTrace software were translated directly into Excel for Windows software for manipulation and on into SPSS for Windows (ver. 21) and JMP 12.0.1 for statistical analyses. In order to evaluate these quantitative determinations, machine data were compared to measurements of known standards during each run. RGM-1 a USGS obsidian standard is analyzed during each sample run for obsidian artifacts to check machine calibration (Table 1). Source assignments were made by reference to Shackley (1995, 2005; Shackley et al. 2018, and updated at http://swxrflab.net/swobsrcs.htm; see Table 1 and Figure 2.

REFERENCES CITED

Davis, K.D., T.L. Jackson, M.S. Shackley, T. Teague, and J.H. Hampel
2011 Factors Affecting the Energy-Dispersive X-Ray Fluorescence (EDXRF) Analysis of Archaeological Obsidian. In *X-Ray Fluorescence Spectrometry (XRF) in Geoarchaeology*, edited by M.S. Shackley, pp. 45-64. Springer, New York.

Govindaraju, K.
1994 1994 Compilation of Working Values and Sample Description for 383 Geostandards. *Geostandards Newsletter* 18 (special issue).

Hampel, Joachim H.
1984 Technical Considerations in X-ray Fluorescence Analysis of Obsidian. In *Obsidian Studies in the Great Basin*, edited by R.E. Hughes, pp. 21-25. Contributions of the University of California Archaeological Research Facility 45. Berkeley.

Hildreth, W.
1981 Gradients in Silicic Magma Chambers: Implications for Lithospheric Magmatism. *Journal of Geophysical Research* 86:10153-10192.

Hughes, Richard E., and Robert L. Smith
1993 Archaeology, Geology, and Geochemistry in Obsidian Provenance Studies. *In Scale on Archaeological and Geoscientific Perspectives*, edited by J.K. Stein and A.R. Linse, pp. 79-91. Geological Society of America Special Paper 283.

Mahood, Gail A., and James A. Stimac
1990 Trace-Element Partitioning in Pantellerites and Trachytes. *Geochemica et Cosmochimica Acta* 54:2257- 2276.

McCarthy, J.J., and F.H. Schamber
1981 Least-Squares Fit with Digital Filter: A Status Report. In *Energy Dispersive X-ray Spectrometry*, edited by K.F.J. Heinrich, D.E. Newbury, R.L. Myklebust, and C.E. Fiori, pp. 273-296. National Bureau of Standards Special Publication 604, Washington, D.C.

Mills, B.J., J.J. Clark, M.A. Peeples, W.R. Haas, Jr., J.M. Roberts, Jr., J.B. Hill, D.L. Huntley, L. Borck, R.L. Breiger, A. Clauset, and M.S. Shackley
2013 Transformation of Social Networks in the Late Pre-Hispanic US Southwest. *PNAS* 110:5785-5790.

Schamber, F.H.
1977 A Modification of the Linear Least-Squares Fitting Method which Provides Continuum Suppression. In *X-ray Fluorescence Analysis of Environmental Samples*, edited by T.G. Dzubay, pp. 241-257. Ann Arbor Science Publishers.

Shackley, M. Steven
1988 Sources of Archaeological Obsidian in the Southwest: An Archaeological, Petrological, and Geochemical Study. *American Antiquity* 53(4):752-772.

1995 Sources of Archaeological Obsidian in the Greater American Southwest: An Update and Quantitative Analysis. *American Antiquity* 60(3):531-551.

1998 Intrasource Chemical Variability and Secondary Depositional Processes in Sources of Archaeological Obsidian: Lessons from the American Southwest. In *Archaeological*

Obsidian Studies: Method and Theory, edited by M.S. Shackley, pp. 83-102. Advances in Archaeological and Museum Studies 3. Springer, New York.

2005 *Obsidian: Geology and Archaeology in the North American Southwest*. University of Arizona Press, Tucson.

2011 An Introduction to X-Ray Fluorescence (XRF) Analysis in Archaeology. In *X-Ray Fluorescence Spectrometry (XRF) in Geoarchaeology*, edited by M.S. Shackley, pp. 7-44. Springer, New York.

2016 Source Provenance Of Obsidian Artifacts From Archaeological Contexts In Southeastern Arizona. Report prepared for Archaeology Southwest and Desert Archaeology, Inc., Tucson.

Shackley, M.S., L.E. Morgan, and D. Pyle
2018 Elemental, Isotopic, and Geochronological Variability in Mogollon-Datil Volcanic Province Archaeological Obsidian, Southwestern USA: Solving Issues of Inter-Source Discrimination. *Geoarchaeology* 33:486-497.

Table 1. Elemental concentrations and source assignments for the archaeological specimens by site, and USGS RGM-1 rhyolite standard. All measurements in parts per million (ppm).

Sample	Ti	Mn	Fe	Zn	Rb	Sr	Y	Zr	Nb	Ba	Pb	Th	Source
220.1A	555	361	7693	45	218	25	40	110	23		24	36	Antelope Cr/Mule Cr
414.1A	802	397	9489	92	260	21	45	115	19		34	43	Antelope Cr/Mule Cr
414.2A	807	386	8895	50	241	24	42	119	25		26	27	Antelope Cr/Mule Cr
414.3A	525	367	7822	74	243	24	40	115	34		26	31	Antelope Cr/Mule Cr
414.4A	649	380	8446	103	248	23	40	115	24		27	38	Antelope Cr/Mule Cr
414.5A	1022	441	6476	77	147	91	24	86	23		20	5	Cow Canyon/111 Ranch
414.6A	641	352	8331	90	248	29	47	113	30		33	35	Antelope Cr/Mule Cr
419.1A	592	378	7451	51	221	19	40	106	27		25	33	Antelope Cr/Mule Cr
419.2A	659	382	8482	47	251	18	46	113	27		29	33	Antelope Cr/Mule Cr
419.3A	13786	375	8496	79	247	22	46	120	28		27	40	Antelope Cr/Mule Cr
419.4A	871	432	9785	60	262	18	46	122	28		36	40	Antelope Cr/Mule Cr
531.1A	1277	437	8016	65	132	126	20	122	9		28	6	Cow Canyon/111 Ranch
710.1A	532	609	7566	100	449	15	78	116	122		37	42	N Sawmill Cr/Mule Cr
751.1A	923	300	6334	34	213	73	22	101	20		25	29	vitrophyre
763.1A	762	444	6321	53	183	12	23	118	32	30	23	32	Mule Mtns/Mule Cr
763.1B	736	370	8864	55	238	22	42	112	31		26	35	Antelope Cr/Mule Cr
981.1A	798	390	9764	83	247	21	43	118	27		31	30	Antelope Cr/Mule Cr
989.1A	519	340	6878	43	215	22	42	107	22		22	28	Antelope Cr/Mule Cr
989.1B	605	364	8327	44	241	18	46	120	26		27	36	Antelope Cr/Mule Cr
1014.1A	613	341	7548	52	235	19	47	117	20		28	35	Antelope Cr/Mule Cr
1115.1A	618	411	9396	48	255	26	50	118	30		34	44	Antelope Cr/Mule Cr
1121.5A	682	365	8505	55	239	24	43	111	23		27	35	Antelope Cr/Mule Cr
1121.5B	607	380	8646	66	244	25	45	118	24		27	28	Antelope Cr/Mule Cr
1207.1A	1230	412	9787	64	202	25	25	101	28	7	30	34	Antelope Cr/Mule Cr?
1207.1B	1437	383	12649	54	241	31	48	126	34		29	43	Antelope Cr/Mule Cr
1207.2A	544	391	8153	46	242	23	40	118	27		32	38	Antelope Cr/Mule Cr
1277.1A	587	352	7911	45	233	23	42	116	27		26	38	Antelope Cr/Mule Cr
1277.1B	778	372	8960	43	232	28	39	118	27		23	26	Antelope Cr/Mule Cr
1277.1C	756	398	9366	53	265	21	46	120	27		33	37	Antelope Cr/Mule Cr
1277.1D	529	340	7483	44	229	21	43	113	27		27	30	Antelope Cr/Mule Cr
1277.1E	569	373	7948	46	241	21	43	116	24		29	34	Antelope Cr/Mule Cr
1277.1F	681	399	9165	51	256	25	46	122	25		31	32	Antelope Cr/Mule Cr
1277.1G	1472	641	10531	74	163	127	30	149	21		23	6	Cow Canyon/111 Ranch
1283.1A	605	356	7820	47	237	23	43	117	32		31	35	Antelope Cr/Mule Cr
1283.1B	612	382	8222	60	240	23	39	110	24		28	40	Antelope Cr/Mule Cr
1283.1C	1376	620	10573	61	163	134	27	154	20		23	17	Cow Canyon/111 Ranch
1283.1D	583	353	7657	46	239	21	45	112	31		28	43	Antelope Cr/Mule Cr
1283.1E	616	441	6339	54	181	14	27	117	39	0	20	29	Mule Mtns/Mule Cr
1283.1F	742	384	9001	47	237	24	43	118	35		26	37	Antelope Cr/Mule Cr
1283.1G	1131	433	7619	42	134	138	20	127	16		22	21	Cow Canyon/111 Ranch
1326.1A	544	394	8043	48	243	21	37	109	28		31	39	Antelope Cr/Mule Cr
1326.1B	1836	455	12039	61	140	138	21	129	15		20	14	Cow Canyon/111 Ranch
1326.1C	636	359	8184	43	240	23	45	121	27		27	25	Antelope Cr/Mule Cr
1326.1D	1510	454	10646	47	135	134	22	129	13	1479	17	13	Cow Canyon/111 Ranch

Sample	Ti	Mn	Fe	Zn	Rb	Sr	Y	Zr	Nb	Ba	Pb	Th	Source
1326.1E	988	400	6940	49	127	126	19	121	12		15	20	Cow Canyon/111 Ranch
1326.1F	1599	462	10303	58	136	131	19	129	14		21	21	Cow Canyon/111 Ranch
1415.1A	626	354	7961	45	237	21	46	116	32		28	34	Antelope Cr/Mule Cr
1415.1B	529	366	7995	45	233	24	44	113	26		28	35	Antelope Cr/Mule Cr
1430.1A	564	391	8930	46	253	23	42	118	32		31	39	Antelope Cr/Mule Cr
1430.1B	981	359	12564	108	273	12	84	251	62	0	25	23	unknown X
1430.1C	866	461	14384	129	309	15	94	274	66	2	33	36	unknown X
1430.1D	968	371	12727	120	270	11	82	250	57	0	32	25	unknown X
1430.1E	828	346	12311	108	283	9	84	245	60	0	27	26	unknown X
1455.1A	543	498	8044	111	111	81	19	82	51		34	5	Government Mtn
1455.2A	987	427	8154	43	156	73	27	78	18	907	23	12	Cow Canyon/111 Ranch
1455.2B	1155	520	8378	60	146	117	20	138	18		20	16	Cow Canyon/111 Ranch
1513.1A	1327	440	8280	58	147	138	19	131	11		20	20	Cow Canyon/111 Ranch
1513.2A	1108	420	8042	69	133	135	21	120	19		21	5	Cow Canyon/111 Ranch
1513.3A	593	356	8486	52	235	23	42	107	28		27	35	Antelope Cr/Mule Cr
1513.4A	1051	396	7280	46	132	133	21	124	10		20	13	Cow Canyon/111 Ranch
1513.5A	626	379	8729	50	243	23	43	116	24		29	33	Antelope Cr/Mule Cr
1513.6A	622	359	8603	55	236	21	41	115	23		28	31	Antelope Cr/Mule Cr
1513.7A	5312	378	8323	75	239	24	44	121	23		31	28	Antelope Cr/Mule Cr
1513.7A	1092	413	10044	81	240	25	45	123	20		28	29	Antelope Cr/Mule Cr
1513.7D	745	404	9156	71	242	23	40	112	28		28	36	Antelope Cr/Mule Cr
1513.7E	676	586	7766	91	438	11	82	113	118		38	49	N Sawmill Cr/Mule Cr
1513.7F	714	362	7842	107	233	21	42	119	29		21	39	Antelope Cr/Mule Cr
1513.7G	750	361	8660	68	237	23	41	114	25		26	31	Antelope Cr/Mule Cr
1513.7G	972	432	7287	62	139	128	21	124	15		18	25	Cow Canyon/111 Ranch
1513.7H	840	353	7909	55	239	25	46	118	26		25	31	Antelope Cr/Mule Cr
1513.7I	1077	371	8935	66	241	22	46	112	25		27	40	Antelope Cr/Mule Cr
1513.7J	723	376	8284	52	242	24	45	120	30		26	43	Antelope Cr/Mule Cr
1513.7K	635	344	8154	58	240	23	41	114	33		27	33	Antelope Cr/Mule Cr
1513.7L	684	379	8525	53	247	23	44	123	25		25	35	Antelope Cr/Mule Cr
RGM1-S4	1558	302	13061	41	148	107	28	222	11	804	22	13	standard
RGM1-S6	1393	310	13170	13	145	108	23	216	10		22	17	standard
RGM1-S6	1435	286	13007	23	143	103	28	217	1		22	17	standard
RGM1-S6	1513	286	12891	14	151	105	25	212	10		24	19	standard

Table 2. Frequency distribution of obsidian source provenance.

		Frequency	Percent
Source	Antelope Cr/Mule Cr	48	64.9
	Antelope Cr/Mule Cr?	1	1.4
	Cow Canyon/111 Ranch	15	20.3
	Government Mtn	1	1.4
	Mule Mtns/Mule Cr	2	2.7
	N Sawmill Cr/Mule Cr	2	2.7
	unknown X	4	5.4
	vitrophyre	1	1.4
	Total	74	100.0

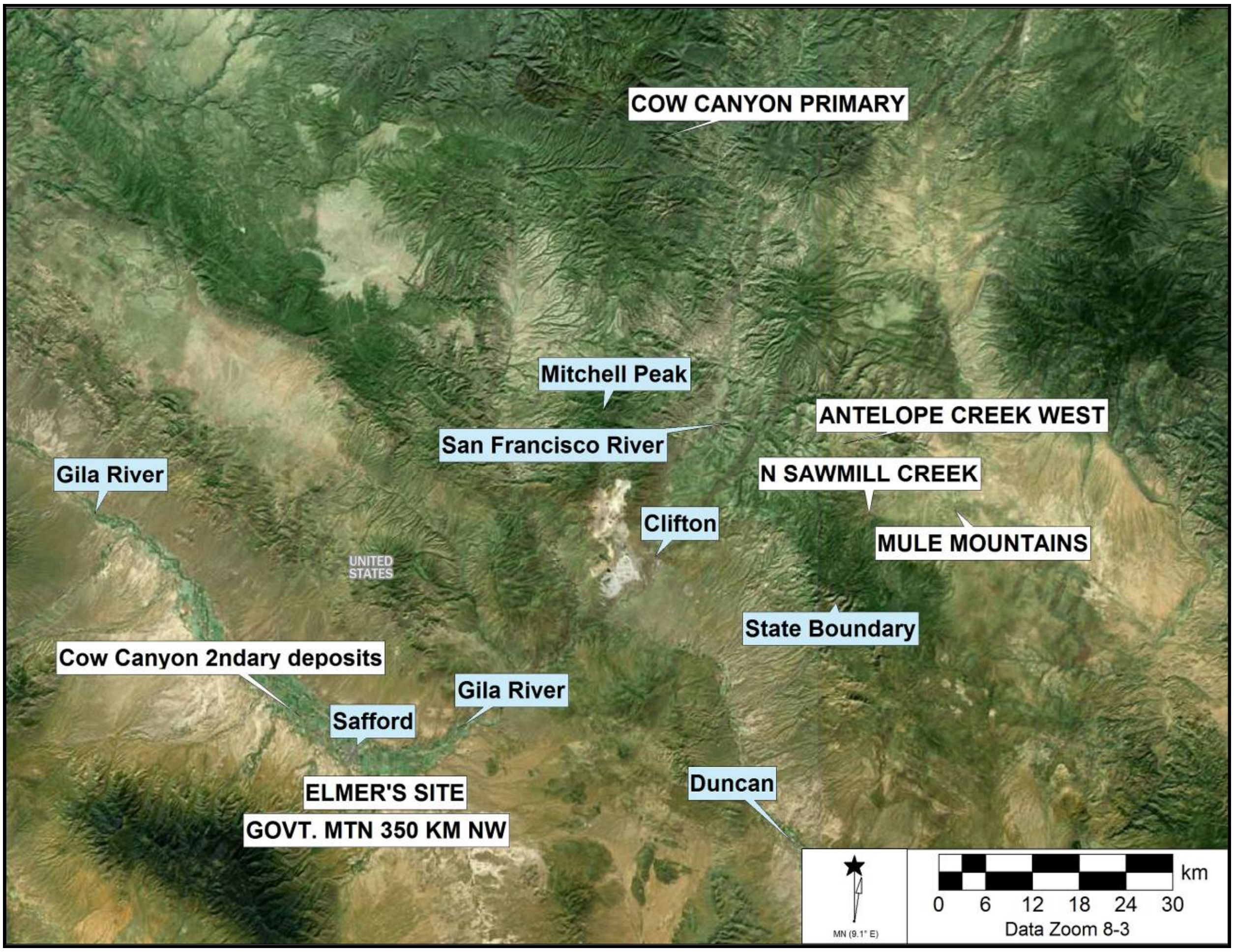

Figure 1. Digital elevation model of site location and relevant obsidian sources.

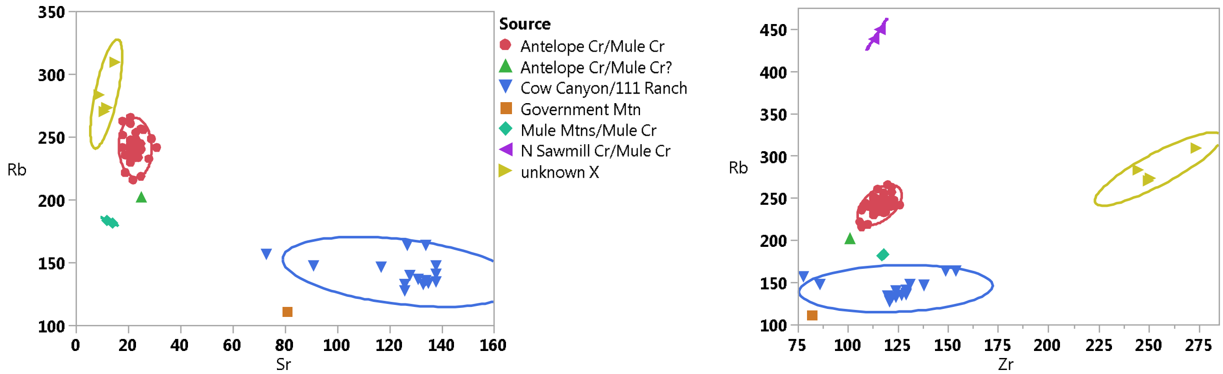

Figure 2. Sr/Rb and Zr/Rb bivariate plots of the archaeological specimens. The high Rb North Sawmill Creek source at Mule Creek omitted in the Sr/Rb plot for clarity. Confidence ellipses at 95%.